




Article

Degradation of Meropenem by Heterogeneous Photocatalysis Using TiO₂/Fiberglass Substrates

Alejandro Altamirano Briones ¹, Iván Córdor Guevara ¹, David Mena ², Isabel Espinoza ², Christian Sandoval-Pauker ³ , Luis Ramos Guerrero ^{1,4}, Paul Vargas Jentsch ^{2,*}  and Florinella Muñoz Bisesti ² 

¹ Departamento de Ciencias de la Tierra y la Construcción, Universidad de las Fuerzas Armadas—ESPE, Av. Gral. Rumiñahui s/n, Sangolquí 171103, Ecuador; gaaltamirano@espe.edu.ec (A.A.B.); ivalexis_14@hotmail.com (I.C.G.); luis.ramos@ute.edu.ec (L.R.G.)

² Departamento de Ciencias Nucleares, Escuela Politécnica Nacional, Ladrón de Guevara E11-253, Quito 170525, Ecuador; david.mena02@epn.edu.ec (D.M.); isabel.espinoza@epn.edu.ec (I.E.); florinella.munoz@epn.edu.ec (F.M.B.)

³ Laboratorio de Fisicoquímica, Departamento de Química, Universidad Técnica Federico Santa María, Avenida España 1680, Valparaíso 2390123, Chile; christian.sandovalp@sansano.usm.cl

⁴ Centro de Investigación de Alimentos_CIAL, Universidad UTE, Av. Mariscal Sucre y Mariana de Jesús, Quito 170527, Ecuador

* Correspondence: paul.vargas@epn.edu.ec; Tel.: +593-2-2976300 (ext. 4231)

Received: 1 March 2020; Accepted: 12 March 2020; Published: 20 March 2020



Abstract: Meropenem (MER), a carbapenem, is considered a last-resort antibiotic. Its presence in water bodies, together with other antibiotics, has brought about environmental problems related to the destruction of natural microorganisms and the development of antibiotic-resistant bacteria. Herein, the degradation of MER by heterogeneous photocatalysis using TiO₂ immobilized on fiberglass substrates is reported. Morphological characterization of the substrates was performed by Scanning Electron Microscopy (SEM). Three pH values (4.0, 5.7, and 7.9) were tested for the treatment of MER solutions (100 mg/L). The best rate constants and MER removals were obtained at pH 4.0 (0.032 min⁻¹; 83.79%) and 5.7 (0.032 min⁻¹; 83.48%). Chemical Oxygen Demand (COD) and Total Organic Carbon (TOC) removals of 25.80% and 29.60% were achieved for the treatment at a pH value of 5.7. The reuse and regeneration of the plates were also tested. The activity of the substrates was maintained until the fourth cycle of reuse, nonetheless, a decrease in MER removal was observed for the 5th cycle. After the fourth cycle of reuse, the activity of the substrates was recovered by a regeneration procedure involving a wash stage of the substrates with a 1% H₂O₂ solution in an ultrasonic bath.

Keywords: meropenem; carbapenem; antibiotics; heterogeneous photocatalysis; titanium dioxide; fiberglass support

1. Introduction

The occurrence of some contaminants of emerging concern (CECs) in the environment has been the focus of intense studies in recent years. The massive use of pharmaceuticals, personal care products, pesticides and others used in everyday life has contributed to the release of this type of compounds into the environment [1]. Among CECs, antibiotics are compounds largely applied to control bacterial infections and allow the treatment of many diseases. Indeed, the development of antibiotics has contributed to reducing mortality and morbidity rates [1,2].

In general, it is a well known fact that pharmaceutical compounds are not completely metabolized, are excreted from the human and/or animal body and then released to the environment [1,3–5]. Moreover, they are not efficiently removed by conventional wastewater treatment plants [6], mostly

due to their chemical structure and antimicrobial characteristics. The presence of antibiotics in the environment has become a public health concern because it has brought environmental effects associated with modifications of the natural microbiota and the emergence of antibiotic-resistant bacteria [7,8].

Carbapenems, such as meropenem (MER), are β -lactam antibiotics that are applied against infections caused by gram-positive and gram-negative bacteria (e.g., *Pseudomonas aeruginosa*) [9,10]. Carbapenems are commonly used as "last-resort antibiotics" when patients are infected by (multi)resistant bacteria or severe infections [11]. Unfortunately, several studies have found bacteria that exhibit resistance also against carbapenems [7,12,13], therefore, proper wastewater treatments for this kind of contaminants are needed to ensure the health safety of future generations.

Advanced Oxidation Processes (AOPs) are a group of treatments that are effective for the removal of persistent organic compounds such as pharmaceuticals, pesticides, solvents, textile dyes, among others. AOPs are based on the generation of highly oxidant species, like hydroxyl radicals ($\bullet\text{OH}$), by different chemical and physicochemical strategies [14,15].

There have been some attempts to application AOPs to remove carbapenem antibiotics reported in the scientific literature. For instance, the application of photo-Fenton processes for the removal of MER using ferrous and persulfate ions was studied [16,17]. Furthermore, the removal of imipenem and MER by direct photolysis under solar irradiation was also tested [11]. To the best of our knowledge, there are really few reports of the application of heterogeneous photocatalysis for the removal of this specific type of antibiotics although its application for the removal of other antibiotics (i.e. amoxicillin, ampicillin, dipyrone, isoniazid, sulfamethoxazole, ciprofloxacin, among others) was extensively reported in the past [18–21]. Therefore, it becomes interesting to assess the feasibility of this type of treatment for the degradation and mineralization of these compounds.

Heterogeneous photocatalysis is based on the adsorption of UV/Vis light on a broadband semiconductor such as TiO_2 [21,22]. When the catalyst absorbs equal or greater energy than its bandgap, an electron from its valence band is promoted to the conduction band generating an electron/hole pair (e^-/h^+). These e^-/h^+ pairs can participate in redox reactions promoting the removal of persistent organic compounds (generally through the formation of $\bullet\text{OH}$ radicals) [19]. This process has some advantages over other AOPs since fewer reagents are required and the catalyst can be separated [21,22].

Generally, the solid photocatalyst can be used in suspension. However, this often represents a disadvantage due to difficulties associated with the separation of the photocatalyst (special filtration systems are needed) and the possible release of nanoparticulate material to the environment. For this reason, the immobilization of TiO_2 on inert materials such as polymers, paint coat, glass, among others is desirable to reduce operational costs [23–25].

Among these materials, fiberglass is a promising support material for metal-based catalysts. Indeed its application as support for platinum and copper-based catalysts has been proven in the past [26,27]. Moreover, the application of this material for the immobilization of TiO_2 was explored in recent works [28–30]. Fiberglass presents some advantages over other traditional materials such as low cost, easy access and high mechanical and thermal stability (even at high temperatures). In addition, its flexibility allows the production of catalysts with different configurations, an aspect that is convenient from the industrial point of view [28,29].

Herein, we report the degradation and mineralization of MER using heterogeneous photocatalysis. In addition, the use of fiberglass as support of TiO_2 is explored. This material support was characterized, and its reuse and regeneration evaluated.

2. Results and Discussion

2.1. Characterization of the TiO_2 /Fiberglass Substrates

In Figure S1 (Supplementary material) are depicted photos of the fiberglass disc before and after the immobilization of TiO_2 . The quantity of TiO_2 immobilized on the substrates was determined by

gravimetric analysis (see Table S1—Supplementary material). On average, 2.1578 ± 0.3319 mg/cm² of TiO₂ were supported on each substrate. It is important to remark that, probably, not all the TiO₂ particles were available for the photocatalysis since a portion of them could be encapsulated by silicone. However, considering that this method of immobilization allowed a stronger retention of particles on the supporting material (fiberglass) compared to other methods (e.g., dip coating), the loss of activity due to the encapsulation of TiO₂ nanoparticles is a minor disadvantage.

SEM images of the TiO₂/fiberglass substrates were obtained to determine the morphological structure of the catalyst (Figure 1). The images showed that TiO₂ was homogeneously distributed over the fiberglass matrix. A certain degree of agglomeration of the catalyst was observed. These agglomerates presented sizes between 200 and 400 nm approximately (see Figure S2—Supplementary material).

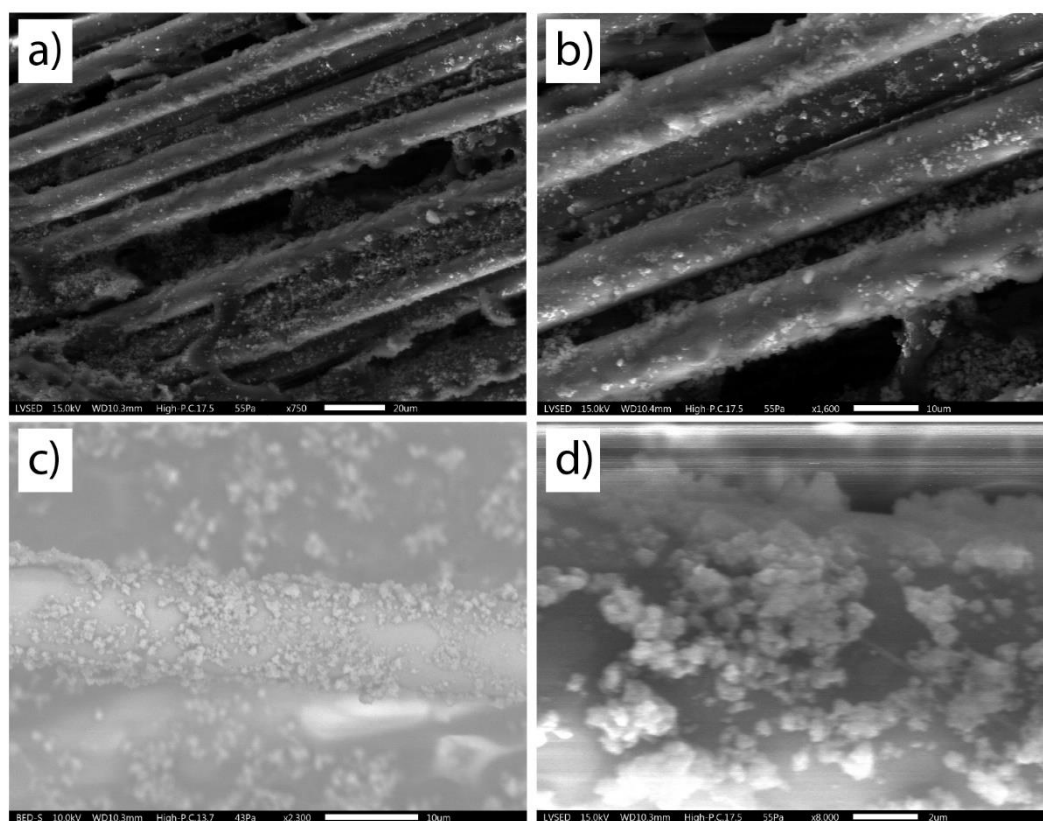
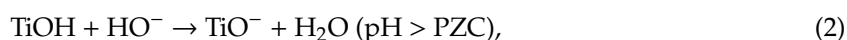
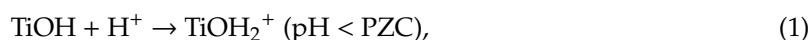


Figure 1. SEM images of the TiO₂/fiberglass substrate (a) 750×; (b) 1600×; (c) 2300×; (d) 8000×.

The determined point of zero charge (PZC) of the substrate is 5.7 (see the plot in Figure S3—Supplementary material) which is close to PZC values reported in other studies for anatase TiO₂ (5.8 to 6.0) [31–33]. The PZC value represents the pH at which the surface of the catalysts has the same number of positive and negative charges. This parameter is used to assess the charge of the catalyst surface and infer whether or not the adsorption can be favored by the pH of the solution. When the pH value is below the PZC, the surface is positively charged, whereas when the pH value is above the PZC, it is negatively charged. In the case of TiO₂, this behavior can be explained with Equations (1) and (2) [24,31]:



2.2. Photocatalytic Removal of Meropenem

The variation of the MER concentration due to the heterogeneous photocatalytic process with TiO₂/fiberglass substrates is depicted in Figure 2. This process was evaluated at three pH values: 4.0,

5.7 and 7.9. The degradation of MER followed a pseudo-first order kinetics according to the coefficients of determination, R^2 (0.933–0.976).

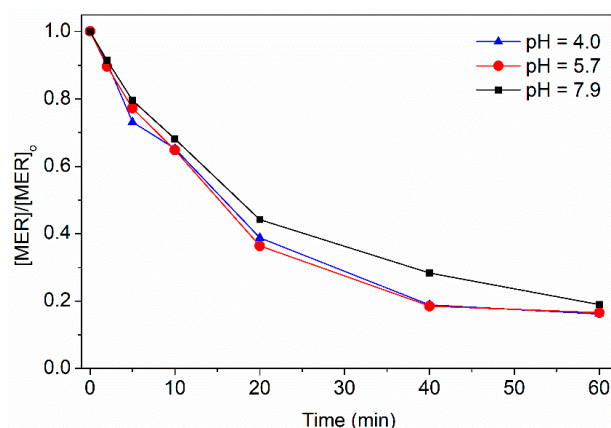


Figure 2. Variation of the MER concentration due to the heterogeneous photocatalytic process with TiO_2 /fiberglass substrates at different pH values ($[\text{MER}]_0 = 100 \text{ mg/L}$).

The pseudo-first order rate constants of the MER photocatalytic degradation calculated for the different pH values tested are depicted in Table 1. A statistical analysis was carried out to determine the effect of the pH value on the removal of MER (Figure S4—Supplementary material) and the results showed that no significant differences between the rate constants at pH 4.0 and 5.7 can be observed. Moreover, a decrease in the rate constant was observed at pH 7.9. The removals of MER attained after 60 min of photocatalytic reaction were 83.79%, 83.48% and 81.05% when the process was carried out at pH 4.0, 5.7 and 7.9, respectively.

Table 1. Pseudo-first order rate constants of the photocatalytic degradation of MER with the TiO_2 /fiberglass substrates at different pH values ($[\text{MER}]_0 = 100 \text{ mg/L}$, $t = 60 \text{ min}$).

pH	$k \text{ (min}^{-1}\text{)}$	R^2
4.0	0.032 ± 0.001	0.946 ± 0.020
5.7	0.032 ± 0.001	0.933 ± 0.009
7.9	0.028 ± 0.001	0.976 ± 0.004

The decrement in the rate constant at a pH value of 7.9 could be explained in terms of the PZC of the substrate and the pK_a values of MER. MER has two pK_a values, the first one (2.9–3.1) is associated with the carbonyl group while the second one (7.4–7.5) is associated with the pyrrolidone group [34]. As mentioned before, the charge of catalyst surface at a specific pH value can be predicted based on the PZC of the material. In this case, when the pH value is above 5.7 (PZC of the material) the adsorption of MER on the substrate is not favored because of the repulsive electrostatic forces between the surface and MER (both are negatively charged). Considering that the adsorption phenomenon is an important step for the photocatalytic degradation of the pollutants [35], a decrease of the adsorption capacity of the material could also affect the photocatalytic performance of the catalyst.

The direct photolysis of MER under UV irradiation was tested. Figure 3 shows the variation of the MER concentration due to the direct photolysis and heterogeneous photocatalysis at pH 5.7. This pH value was selected by considering the results of the photocatalytic degradation of MER. Taking into consideration that no significant differences between the treatments carried out at pH 4.0 and 5.7 were observed, a pH value of 5.7 was selected for the treatment since it implies a lower operational costs at an industrial scale (less acid is required to adjust the pH). The photolysis experiments showed that MER can be degraded by direct photolysis, as reported previously [11]. Indeed, a MER removal of 66.44% was achieved after 60 min of reaction. Nevertheless, when the substrate was employed, an

improvement on the degradation of MER was observed. For comparative purposes, the degradation of MER by direct photolysis was adjusted to pseudo-first order kinetics ($k = 0.0189 \text{ min}^{-1}$ and $R^2 = 0.992$).

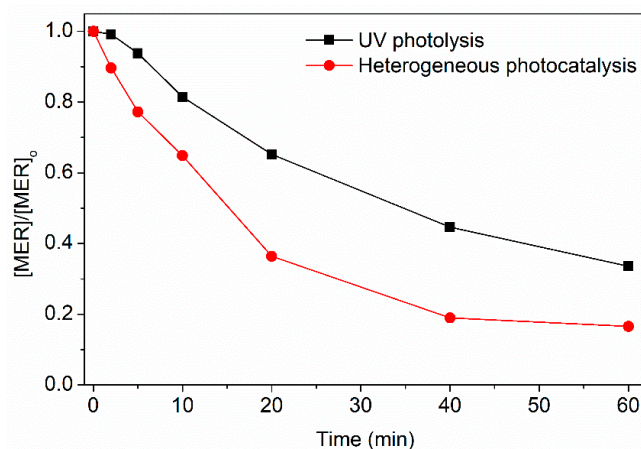


Figure 3. Variation of the MER concentration due to UV photolysis and heterogeneous photocatalysis with the $\text{TiO}_2/\text{fiberglass}$ substrate ($[\text{MER}]_0 = 100 \text{ mg/L}$, $\text{pH} = 5.7$).

The adsorption of MER over the $\text{TiO}_2/\text{fiberglass}$ substrates at $\text{pH} = 5.7$ was also studied. According to the results, the time required to attain the adsorption equilibria was 10 min. Moreover, Langmuir and Freundlich isotherm models were applied to describe the adsorption data. Based on the coefficients of determination a better fit was found with the Langmuir model ($R^2 = 0.925$). The maximum adsorption capacity (q_{max}) and the Langmuir constant (K_L) calculated for the MER adsorption were 0.052 mg/g and 0.073 L/mg , respectively.

2.3. Mineralization and Biodegradability Studies

The mineralization of MER by the photocatalytic treatment was studied in terms of chemical oxygen demand (COD) and total organic carbon (TOC). These experiments were conducted with an initial MER concentration of 100 mg/L , a pH value of 5.7 and 60 min of reaction. COD and TOC removals of 25.80% and 29.60% were achieved, respectively. These results suggest that the treatment could trigger the formation of less complex species. Nevertheless, the low COD and TOC removals in comparison to the removal of MER (83.79%) may be explained by the presence of different reaction intermediates which do not easily degraded in comparison with MER molecules [17,36].

2.4. Reuse and Regeneration of the Material

One of the main drawbacks of the application of heterogeneous photocatalysis is the deactivation of the catalysts generally due to the adsorption of the pollutant and/or its degradation products. For industrial purposes, it is desirable that the photocatalysts can be reused and/or regenerated. In this sense, the recyclability of the substrates was studied. The substrates were reused for five subsequent cycles of MER degradation. Figure 4 shows the MER photocatalytic degradation kinetics for each cycle. The activity of the substrates was slightly affected until the fourth cycle of reuse. However, a decrease in MER removal was observed during the fifth cycle (see Figure S5—Supplementary material). Other studies have also reported the progressive fouling of TiO_2 after several uses [37–40].

After the fifth cycle of reuse, a simple regeneration method for the substrates was tested. This regeneration process consisted of washing the substrates with a 1% H_2O_2 solution in an ultrasonic bath for 15 min and drying them at $80 \text{ }^\circ\text{C}$ for 5 h. Then, the regenerated substrate was employed for another MER degradation cycle. The results demonstrate that this simple procedure can restore the activity of the substrates (see Figure S5—Supplementary material). The regeneration of the catalyst could not only be explained by the removal of the substances adsorbed on the surface of the substrate by washing. Perhaps, the combined action of ultrasound irradiation and H_2O_2 (which is a well-known

advanced oxidation process) can generate $\bullet\text{OH}$ radicals which could oxidize the adsorbed pollutants and thus facilitate their desorption. Other works have also proven the capacity of H_2O_2 to aid in the regeneration process of photocatalysts [40]. The reuse and regeneration of the substrates make them suitable for industrial wastewater applications by reducing the cost of the treatment and the amount of the spent catalyst discarded to the environment.

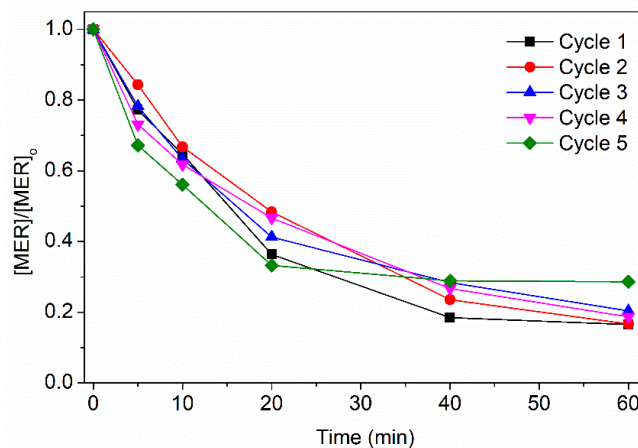


Figure 4. Photocatalytic degradation kinetics of MER obtained for the 5 cycles of reuse of the TiO_2 /fiberglass substrates ($[\text{MER}]_0 = 100 \text{ mg/L}$, $\text{pH} = 5.7$).

3. Materials and Methods

3.1. Reagents

Meropenem trihydrate was purchased from Chongqing Pharmaceutical (71.6% meropenem; impurities were 7.1% NaCl, 100 ppm acetone, 500 ppm ethanol, 1000 ppm isopropanol, <10 ppm metals, and water). Nanosized titanium dioxide (TiO_2) was provided by Nanostructured and Amorphous Materials Inc. (size of grain 15 nm, 99% anatase). Moreover, tetrabutylammonium hydroxide (20%), acetonitrile (LiChrosolv®) and methanol (LiChrosolv®) were bought from Merck. Phosphoric acid (85%) was obtained from Fisher. The structure of Meropenem (MER) is provided in Figure 5.

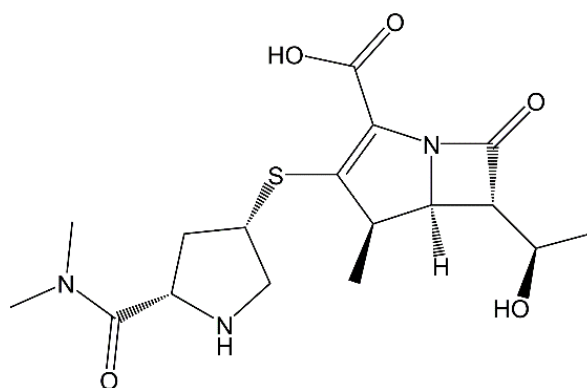


Figure 5. Chemical structure of MER ($\text{C}_{17}\text{H}_{25}\text{N}_3\text{O}_5\text{S}$; (4R,5S,6S)-3-[(3S,5S)-5-(dimethylcarbamoyl)pyrrolidin-3-yl]sulfanyl-6-[(1R)-1-hydroxyethyl]-4-methyl-7-oxo-1-azabicyclo[3.2.0]hept-2-ene-2-carboxylic acid).

3.2. Preparation of TiO_2 /Fiberglass Substrates

TiO_2 was immobilized on a fiberglass disc with an inner and outer diameter of 20 and 80 mm, respectively. Before the immobilization, the discs were washed with ethanol (50% *v/v*) and sonicated for 5 min. Subsequently, they were dried at 100°C for 24 h. To guarantee a homogeneous weight distribution, only the discs with a mass of $1.8 \pm 0.2 \text{ g}$ were selected as support for the photocatalyst.

For the immobilization of TiO₂, 0.75 g of liquid silicone was mixed with 15 mL of ethanol (96% *v/v*) at constant stirring. Once dissolved, 0.25 g of TiO₂ were added and stirred for 5 min. Then, the TiO₂ suspension was carefully spilled onto the fiberglass discs, spread to achieve a uniform distribution and then dried at 80 °C for 24 h. The amount of catalyst present in the prepared substrates was determined by gravimetric analysis using an analytical balance (CX220 Citizen).

The point of zero charge (PZC) of the TiO₂/fiberglass substrates was determined using a methodology previously described [31,41]. For the morphological characterization, the prepared substrates were analyzed by a Scanning Electron Microscope (JEOL, Model: JSM-IT300).

3.3. Photocatalytic Degradation of Meropenem

Photocatalytic assays were carried out with solutions of MER (100 mg/L). The solutions were treated in a batch lab-scale system which consisted of a stirred reaction vessel, two UV lamps (8 W) and a cooling system to maintain the temperature at approximately 20 °C. The TiO₂/fiberglass substrates were submerged into 25 mL of MER solutions. Then, the solutions were stirred for 35 min in the darkness (to ensure the adsorption equilibria). After the pre-equilibration step, the lamp was turned on to start the photocatalytic reaction. The tests were performed at different times of reaction (0, 2, 5, 10, 20, 40, 60 min) and three pH values (4.0, 5.7 and 7.9). A clean substrate was employed for each assay. The pH value that allowed the highest MER removal was chosen for further experiments. Moreover, to measure the degree in which MER can be degraded due to photolysis, MER solutions (100 mg/L) were irradiated without the substrates.

After each run, the remaining MER in the solutions (concentration) was measured by HPLC (Agilent Technologies 1120 compact LC) equipped with a variable wavelength UV-Vis detector and a Zorbax Eclipse Plus C-18 column from Agilent Technologies (4.6 mm × 150 mm; 5 μm particle size). The mobile phase consisted of a mixture of methanol, acetonitrile, and a buffer solution of tetrabutylammonium hydroxide adjusted to a pH of 7.0 with phosphoric acid (volume ratio 10:15:75). The flow rate of the mobile phase was set to 1.5 mL/min with an isocratic regime. The detection was carried out at 300 nm.

In addition, the adsorption of MER on the TiO₂/fiberglass substrates was evaluated. The equilibrium time of adsorption was first determined. The substrates were submerged in 25 mL of MER solutions (20 mg/L) with stirring at 200 rpm in the absence of light. The assays were carried out at different times (5, 10, 20, 30, 40, 50 min). For each assay, the remaining MER in the solutions was measured by HPLC.

Once the equilibrium time was determined, the adsorption isotherm of MER on the substrates was obtained at room temperature (~18 °C). For this, the TiO₂/fiberglass substrates were submerged in 25 mL of MER solutions (40, 50, 60, 70, 80, 100 mg/L) with stirring at 200 rpm in the absence of light until the adsorption equilibrium was reached. The concentration of MER after the tests was measured by HPLC. The resulting adsorption isotherm was adjusted to the linear form of Langmuir and Freundlich models which are presented in Equations (3) and (4), respectively [42].

$$C_e/q_e = 1/(K_L \cdot q_{\max}) + C_e/q_{\max} \quad (3)$$

$$\ln(q_e) = 1/n \cdot \ln(C_e) + \ln(K_F) \quad (4)$$

where C_e is the equilibrium concentration (mg/L), q_e is the equilibrium amount of MER adsorbed on the substrate (mg/g), q_{\max} is the maximum adsorption capacity of the substrate (mg/g), K_L (L/mg) is the Langmuir constant, K_F ($\text{mg}^{1-n} \cdot \text{L}^n \cdot \text{g}^{-1}$) is the Freundlich constant, and $1/n$ is a constant related to the intensity of the adsorption in the Freundlich model.

3.4. Mineralization of MER

The mineralization of MER was studied in terms of the chemical oxygen demand (COD) and total organic carbon (TOC). For this, MER solutions (100 mg/L) were treated using the TiO₂/fiberglass

substrate. After 60 min of treatment, COD and TOC were measured according to the standard methods 5220 D and 5310 B, respectively [43].

3.5. Reuse and Regeneration of the TiO₂/Fiberglass Substrates

The reuse and regeneration of the TiO₂/fiberglass substrates were studied. Five subsequent cycles of (re)use were carried out using the same substrate. For these assays, portions of 25 mL of MER solutions (100 mg/L) were treated for 60 min. After the treatment, the used substrate was separated and dried at room temperature before its reuse in another treatment (this procedure was repeated four times). Additionally, after the fifth cycle, the substrates were regenerated and employed for an additional degradation run. The regeneration process consisted of washing the substrates with a 1% H₂O₂ solution in an ultrasonic bath for 15 min and then drying them at 80 °C for 5 h.

4. Conclusions

The degradation and mineralization of MER using TiO₂/fiberglass substrates as heterogeneous photocatalysts were studied. The photocatalysts were prepared by immobilizing TiO₂ on a fiberglass matrix. The morphology of the substrates was characterized by Scanning Electron Microscopy. A homogeneous distribution of TiO₂ over the fiberglass matrix was observed by SEM. The quantity of TiO₂ immobilized on the plates was on average 2.1578 ± 0.3319 mg/cm². The photocatalytic degradation of MER was carried out at three pH values (4.0, 5.7 and 7.9). The statistical analysis showed that there were no significant statistical differences between the rate constants at pH 4.0 and 5.7 (0.032 min⁻¹ in both cases). Nevertheless, a decrease in the rate constant was observed at pH 7.9 (0.028 min⁻¹). The direct photolysis of MER with UV light was also tested. The rate constant for the photolysis of MER was 0.0189 min⁻¹ which was lower than the rate constant of the photocatalysis. Thus, the addition of the substrates had a positive effect on the removal of this compound. The adsorption isotherm of MER on the substrates was adjusted to the Langmuir model with a maximum adsorption capacity (q_{\max}) and Langmuir constant (K_L) of 0.052 mg/g and 0.073 L/mg, respectively. To provide insight into the mineralization of MER by the treatment, COD and TOC parameters were measured. COD and TOC removals were 25.80% and 29.60%, respectively. These values suggest that the treatment could trigger the formation of a less complex species. Moreover, the reuse and regeneration of the substrates were studied. For this, the substrates were reused for five subsequent cycles of MER degradation, the activity of the substrates was maintained until the fourth cycle of reuse. However, a decrease in MER removal was observed during the fifth cycle. After the fifth cycle of reuse, the activity of the substrates was recovered by the regeneration procedure.

Supplementary Materials: The following are available online at <http://www.mdpi.com/2073-4344/10/3/344/s1>, Table S1: Average content of TiO₂ immobilized on the fiberglass substrates, Figure S2: SEM images of the TiO₂/fiberglass substrate, Figure S3: Point of zero charge of the TiO₂/fiberglass substrate, Figure S4: Statistical analysis of the effect of the pH value on the pseudo-first order rate constant of the photocatalytic degradation meropenem, Figure S5: Statistical analysis of the effect of the reuse of the TiO₂/fiberglass substrate on the removal of MER after 60 min of reaction (pH = 5.7).

Author Contributions: A.A.B. and I.C.G. prepared the photocatalysts, characterize them and tested their activity; D.M. develop the methodology for the preparation of the substrates; the manuscript was written and drafted by I.E. and C.S.-P.; L.R.G., P.V.J. and F.M.B. designed the experiments, played a supervising role and review and edit the final version of the manuscript. All authors have read and agreed to the published version of the manuscript.

Funding: This research received no external funding. The APC was funded by Escuela Politécnica Nacional.

Acknowledgments: The authors thank the support provided by Universidad de las Fuerzas Armadas—ESPE, Escuela Politécnica Nacional and Universidad UTE. A.A.B., I.C.G. and D.M. are grateful to Paola Zarate Pozo from Departamento de Ciencias Nucleares of Escuela Politécnica Nacional for providing support in the HPLC measurements.

Conflicts of Interest: The authors declare no conflict of interest.

References

1. Carvalho, I.T.; Santos, L. Antibiotics in the aquatic environments: A review of the European scenario. *Environ. Int.* **2016**, *94*, 736–757. [[CrossRef](#)] [[PubMed](#)]
2. Vardanyan, R.; Hruby, V. *Synthesis of Best-Seller Drugs*, 1st ed.; Elsevier: Amsterdam, The Netherland, 2016.
3. Grenni, P.; Ancona, V.; Barra Caracciolo, A. Ecological effects of antibiotics on natural ecosystems: A review. *Microchem. J.* **2018**, *136*, 25–39. [[CrossRef](#)]
4. Liu, X.; Lu, S.; Guo, W.; Xi, B.; Wang, W. Antibiotics in the aquatic environments: A review of lakes, China. *Sci. Total Environ.* **2018**, *627*, 1195–1208. [[CrossRef](#)] [[PubMed](#)]
5. Yang, Y.; Song, W.; Lin, H.; Wang, W.; Du, L.; Xing, W. Antibiotics and antibiotic resistance genes in global lakes: A review and meta-analysis. *Environ. Int.* **2018**, *116*, 60–73. [[CrossRef](#)] [[PubMed](#)]
6. Alexander, J.; Knopp, G.; Dötsch, A.; Wieland, A.; Schwartz, T. Ozone treatment of conditioned wastewater selects antibiotic resistance genes, opportunistic bacteria, and induce strong population shifts. *Sci. Total Environ.* **2016**, *559*, 103–112. [[CrossRef](#)]
7. Hrenovic, J.; Ivankovic, T.; Ivekovic, D.; Repec, S.; Stipanicev, D.; Ganjto, M. The fate of carbapenem-resistant bacteria in a wastewater treatment plant. *Water Res.* **2017**, *126*, 232–239. [[CrossRef](#)]
8. Szekeres, E.; Baricz, A.; Chiriac, C.M.; Farkas, A.; Opris, O.; Soran, M.-L.; Andrei, A.-S.; Rudi, K.; Balcázar, J.L.; Dragos, N.; et al. Abundance of antibiotics, antibiotic resistance genes and bacterial community composition in wastewater effluents from different Romanian hospitals. *Environ. Pollut.* **2017**, *225*, 304–315. [[CrossRef](#)]
9. Kongthavonsakul, K.; Lucksiri, A.; Eakanunkul, S.; Roongjang, S.; Issarangoon na Ayuthaya, S.; Oberdorfer, P. Pharmacokinetics and pharmacodynamics of meropenem in children with severe infection. *Int. J. Antimicrob. Agents* **2016**, *48*, 151–157. [[CrossRef](#)]
10. Proia, L.; Anzil, A.; Borrego, C.; Farrè, M.; Llorca, M.; Sanchis, J.; Bogaerts, P.; Balcázar, J.L.; Servais, P. Occurrence and persistence of carbapenemases genes in hospital and wastewater treatment plants and propagation in the receiving river. *J. Hazard. Mater.* **2018**, *358*, 33–43. [[CrossRef](#)]
11. Reina, A.C.; Martínez-Piarnas, A.B.; Bertakis, Y.; Brebou, C.; Xekoukoulotakis, N.P.; Agüera, A.; Sánchez Pérez, J.A. Photochemical degradation of the carbapenem antibiotics imipenem and meropenem in aqueous solutions under solar radiation. *Water Res.* **2018**, *128*, 61–70. [[CrossRef](#)]
12. Khan, A.; Sharma, D.; Faheem, M.; Bisht, D.; Khan, A.U. Proteomic analysis of a carbapenem-resistant *Klebsiella pneumoniae* strain in response to meropenem stress. *J. Glob. Antimicrob. Resist.* **2017**, *8*, 172–178. [[CrossRef](#)] [[PubMed](#)]
13. Magalhães, M.J.T.L.; Pontes, G.; Serra, P.T.; Balieiro, A.; Castro, D.; Pieri, F.A.; Crainey, J.L.; Nogueira, P.A.; Orlandi, P.P. Multidrug resistant *Pseudomonas aeruginosa* survey in a stream receiving effluents from ineffective wastewater hospital plants. *BMC Microbiol.* **2016**, *16*, 193. [[CrossRef](#)] [[PubMed](#)]
14. Dewil, R.; Mantzavinos, D.; Poullos, I.; Rodrigo, M.A. New perspectives for Advanced Oxidation Processes. *J. Environ. Manag.* **2017**, *195*, 93–99. [[CrossRef](#)] [[PubMed](#)]
15. Gagol, M.; Przyjazny, A.; Boczkaj, G. Wastewater treatment by means of advanced oxidation processes based on cavitation—A review. *Chem. Eng. J.* **2018**, *338*, 599–627. [[CrossRef](#)]
16. Kordestani, B.; Takdastan, A.; Jalilzadeh Yengejeh, R.; Neisi, A.K. Photo-Fenton oxidative of pharmaceutical wastewater containing meropenem and ceftriaxone antibiotics: Influential factors, feasibility, and biodegradability studies. *Toxin Rev.* **2018**, *1*–11. [[CrossRef](#)]
17. Kordestani, B.; Jalilzadeh Yengejeh, R.; Takdastan, A.; Neisi, A.K. A new study on photocatalytic degradation of meropenem and ceftriaxone antibiotics based on sulfate radicals: Influential factors, biodegradability, mineralization approach. *Microchem. J.* **2019**, *146*, 286–292. [[CrossRef](#)]
18. Giri, A.S.; Golder, A.K. Fenton, Photo-Fenton, H₂O₂ Photolysis, and TiO₂ Photocatalysis for Dipyron Oxidation: Drug Removal, Mineralization, Biodegradability, and Degradation Mechanism. *Ind. Eng. Chem. Res.* **2014**, *53*, 1351–1358. [[CrossRef](#)]
19. Elmolla, E.S.; Chaudhuri, M. Photocatalytic degradation of amoxicillin, ampicillin and cloxacillin antibiotics in aqueous solution using UV/TiO₂ and UV/H₂O₂/TiO₂ photocatalysis. *Desalination* **2010**, *252*, 46–52. [[CrossRef](#)]
20. Malesic-Eleftheriadou, N.; Evgenidou, E.N.; Kyzas, G.Z.; Bikiaris, D.N.; Lambropoulou, D.A. Removal of antibiotics in aqueous media by using new synthesized bio-based poly(ethylene terephthalate)-TiO₂ photocatalysts. *Chemosphere* **2019**, *234*, 746–755. [[CrossRef](#)] [[PubMed](#)]

21. Silva, A.R.; Martins, P.M.; Teixeira, S.; Carabineiro, S.A.C.; Kuehn, K.; Cuniberti, G.; Alves, M.M.; Lanceros-Mendez, S.; Pereira, L. Ciprofloxacin wastewater treated by UVA photocatalysis: Contribution of irradiated TiO₂ and ZnO nanoparticles on the final toxicity as assessed by *Vibrio fischeri*. *RSC Adv.* **2016**, *6*, 95494–95503. [[CrossRef](#)]
22. Babić, S.; Ćurković, L.; Ljubas, D.; Čizmić, M. TiO₂ assisted photocatalytic degradation of macrolide antibiotics. *Curr. Opin. Green Sustain. Chem.* **2017**, *6*, 34–41. [[CrossRef](#)]
23. Sousa, V.M.; Manaia, C.M.; Mendes, A.; Nunes, O.C. Photoinactivation of various antibiotic resistant strains of *Escherichia coli* using a paint coat. *J. Photochem. Photobiol. A Chem.* **2013**, *251*, 148–153. [[CrossRef](#)]
24. Sandoval, C.; Molina, G.; Vargas Jentsch, P.; Pérez, J.; Muñoz, F. Photocatalytic Degradation of Azo Dyes Over Semiconductors Supported on Polyethylene Terephthalate and Polystyrene Substrates. *J. Adv. Oxid. Technol.* **2017**, *20*. [[CrossRef](#)]
25. Huang, C.; Ding, Y.; Chen, Y.; Li, P.; Zhu, S.; Shen, S. Highly efficient Zr doped-TiO₂/glass fiber photocatalyst and its performance in formaldehyde removal under visible light. *J. Environ. Sci.* **2017**, *60*, 61–69. [[CrossRef](#)]
26. Balandina, T.A.; Larina, T.Y.; Kuznetsova, N.I.; Bal'zhinimaev, B.S. Copper catalysts based on fiberglass supports for hydrocarbon oxidation reactions with the participation of hydrogen peroxide. *Kinet. Catal.* **2008**, *49*, 499–505. [[CrossRef](#)]
27. Bal'zhinimaev, B.S.; Kovalyov, E.V.; Kaichev, V.V.; Suknev, A.P.; Zaikovskii, V.I. Catalytic Abatement of VOC Over Novel Pt Fiberglass Catalysts. *Top. Catal.* **2017**, *60*, 73–82. [[CrossRef](#)]
28. Brichkov, A.S.; Shamsutdinova, A.N.; Khalipova, O.S.; Rogacheva, A.O.; Larina, T.V.; Glazneva, T.S.; Cherepanova, S.V.; Paukshtis, E.A.; Buzaev, A.A.; Kozik, V.V.; et al. Preparation of a fiberglass-supported Ni-Si-Ti oxide catalyst for oxidation of hydrocarbons: Effect of SiO₂. *J. Chem. Technol. Biotechnol.* **2019**, *94*, 3618–3624. [[CrossRef](#)]
29. Sun, P.; Xue, R.; Zhang, W.; Zada, I.; Liu, Q.; Gu, J.; Su, H.; Zhang, Z.; Zhang, J.; Zhang, D. Photocatalyst of organic pollutants decomposition: TiO₂/glass fiber cloth composites. *Catal. Today* **2016**, *274*, 2–7. [[CrossRef](#)]
30. Wang, M.; Chen, W.; Liu, C. The Preparation of TiO₂ Film Loaded on Fiberglass Mesh and the Experimental Study on Its Photocatalytic Properties. *Adv. Mater. Res.* **2010**, *150*, 1421–1424. [[CrossRef](#)]
31. Sriprang, P.; Wongnawa, S.; Sirichote, O. Amorphous titanium dioxide as an adsorbent for dye polluted water and its recyclability. *J. Sol-Gel Sci. Technol.* **2014**, *71*, 86–95. [[CrossRef](#)]
32. Kosmulski, M. The significance of the difference in the point of zero charge between rutile and anatase. *Adv. Colloid Interface Sci.* **2002**, *99*, 255–264. [[CrossRef](#)]
33. Vu, D.; Li, Z.; Zhang, H.; Wang, W.; Wang, Z.; Xu, X.; Dong, B.; Wang, C. Adsorption of Cu(II) from aqueous solution by anatase mesoporous TiO₂ nanofibers prepared via electrospinning. *J. Colloid Interface Sci.* **2012**, *367*, 429–435. [[CrossRef](#)] [[PubMed](#)]
34. Çubuk Demiralay, E.; Koç, D.; Daldal, Y.D.; Alsancak, G.; Ozkan, S.A. Determination of chromatographic dissociation constants of some carbapenem group antibiotics and quantification of these compounds in human urine. *Biomed. Chromatogr.* **2014**, *28*, 660–666. [[CrossRef](#)] [[PubMed](#)]
35. Picho-Chillán, G.; Dante, R.C.; Muñoz-Bisesti, F.; Martín-Ramos, P.; Chamorro-Posada, P.; Vargas-Jentsch, P.; Sánchez-Arévalo, F.M.; Sandoval-Pauker, C.; Rutto, D. Photodegradation of Direct Blue 1 azo dye by polymeric carbon nitride irradiated with accelerated electrons. *Mater. Chem. Phys.* **2019**, *237*, 121878. [[CrossRef](#)]
36. Parsa, J.B.; Golmirzaei, M.; Abbasi, M. Degradation of azo dye C.I. Acid Red 18 in aqueous solution by ozone-electrolysis process. *J. Ind. Eng. Chem.* **2014**, *20*, 689–694. [[CrossRef](#)]
37. Chekem, C.T.; Richardson, Y.; Drobek, M.; Plantard, G.; Blin, J.; Goetz, V. Effective coupling of phenol adsorption and photodegradation at the surface of micro- and mesoporous TiO₂-activated carbon materials. *React. Kinet. Mech. Catal.* **2017**, *122*, 1297–1321. [[CrossRef](#)]
38. Lin, L.; Wang, H.; Luo, H.; Xu, P. Enhanced photocatalysis using side-glowing optical fibers coated with Fe-doped TiO₂ nanocomposite thin films. *J. Photochem. Photobiol. A Chem.* **2015**, *307*, 88–98. [[CrossRef](#)]
39. Meng, A.; Xing, J.; Guo, W.; Li, Z.; Wang, X. Electrospinning synthesis of porous Bi₁₂TiO₂₀/Bi₄Ti₃O₁₂ composite nanofibers and their photocatalytic property under simulated sunlight. *J. Mater. Sci.* **2018**, *53*, 14328–14336. [[CrossRef](#)]
40. Wu, H.S.; Wang, Y.L. Inactivation and Regeneration of Photocatalytic Properties of ZnO Nanofilm Materials. *Adv. Mater. Res.* **2012**, *531*, 199–202. [[CrossRef](#)]

41. Newcombe, G.; Hayes, R.; Drikas, M. Granular activated carbon: Importance of surface properties in the adsorption of naturally occurring organics. *Colloids Surfaces A Physicochem. Eng. Asp.* **1993**, *78*, 65–71. [[CrossRef](#)]
42. Darwish, A.A.A.; Rashad, M.; AL-Aoh, H.A. Methyl orange adsorption comparison on nanoparticles: Isotherm, kinetics, and thermodynamic studies. *Dyes Pigments* **2019**, *160*, 563–571. [[CrossRef](#)]
43. Baird, R.B.; Eaton, A.D.; Rice, E.W. *Standard Methods for the Examination of Water and Wastewater*, 23rd ed.; American Public Health Association, American Water Works Association, Water Environment Federation: Washington, DC, USA, 2017.



© 2020 by the authors. Licensee MDPI, Basel, Switzerland. This article is an open access article distributed under the terms and conditions of the Creative Commons Attribution (CC BY) license (<http://creativecommons.org/licenses/by/4.0/>).